Probing the shear viscosity of an active nematic film

Pau Guillamat, Jordi Ignés-Mullol, Suraj Shankar, M. Cristina Marchetti, and Francesc Sagués

Phys. Rev. E **94**, 060602 — Published 28 December 2016

DOI: 10.1103/PhysRevE.94.060602

Probing the shear viscosity of an active nematic

Pau Guillamat[a], Jordi Ignés-Mullol[a], Suraj Shankar[b], M. Cristina Marchetti[b], and Francesc Sagués[a*]
[a] *Departament de Química Física and Institute of Nanoscience and Nanotechnology (IN2UB), Universitat de Barcelona, Martí i Franquès 1, 08028 Barcelona, Catalonia, Spain.*
[b] *Physics Department and Syracuse Soft Matter Program, Syracuse University, Syracuse, NY 13244, USA.*
(Dated: December 12, 2016)

In vitro reconstituted active systems, such as the ATP-driven microtubule bundle suspension developed by the Dogic group, provide a fertile testing ground for elucidating the phenomenology of active liquid crystalline states. Controlling such novel phases of matter crucially depends on our knowledge of their material and physical properties. In this letter, we show that the shear viscosity of an active nematic film can be probed by varying its hydrodynamic coupling to a bounding oil layer. Using the motion of disclinations as intrinsic tracers of the flow field and a hydrodynamic model, we obtain an estimate for the as of now unknown shear viscosity of the nematic film. Knowing this now provides us with an additional handle for robust and precision tunable control of the emergent dynamics of active fluids.

PACS numbers: 87.16.Ka,61.30.Jf,83.85.Jn

Active systems are collections of self-propelling entities that display non-equilibrium self-organization on many scales [1, 2]. Examples from the living world include animal flocks [3], bacterial colonies [4, 5], living tissues and cytoskeletal extracts [6–8]. Ingenious synthetic analogues composed either of externally driven [9–11] or autonomously propelled elements [12–14] have also been developed. The distinctive feature that unifies these systems is that they are composed of interacting units that convert ambient or stored energy into self-sustained motion, from coherently organized to seemingly chaotic.

In many experimental realizations, active fluids are composed of elongated units and exhibit liquid crystalline order. While a lot of previous work has highlighted the complex nonequilibrium dynamics of these systems and the novel properties of topological defects that themselves become dynamical entities capable of driving the motion [15, 16], the material properties of active gels remain largely unexplored. A few studies have probed the shear viscosity of suspensions of micro-organisms [17–20], with remarkable results. In particular, it was shown that activity decreases the effective viscosity of a suspension of *E. coli*, driving it to zero or even negative values [20, 21], in agreement with early theoretical predictions [22–24]. More subtle, however, is the behavior of active nematic liquid crystals composed of head-tail symmetric units that exert active forces on their surroundings, but exhibit no mean motion. Much interest in this class of active fluids has been fuelled by the group of Z. Dogic [8, 25] who has pioneered a remarkable model active nematic consisting of a suspension of microtubules (MTs) in the presence of Adenosin Triphosphate (ATP)-fuelled kinesin motors. Bundled MTs behave as active units that exert extensile forces on their environment and are capable of reproducing *in vitro* some of the unique behavior of living systems. When concentrated at an oil-water interface, the suspension of MT bundles organizes into an active nematic that exhibits self-sustained spontaneous flows with striking resemblance to the streaming used by cells to circulate their fluid content. At high enough activity active turbulent flows develop, with proliferation of unbound disclinations - the distinctive textures of two-dimensional films of nematic liquid crystals. By confining the suspension of MTs to the surface of a lipid vesicle, Keber *et al.* fabricated "active vesicles" that can undergo spontaneous oscillations and remarkable shape changes [26]. Reconstituted suspensions of cytoskeletal filaments and associated motor proteins serve as ideal model systems for understanding subcellular organization. Extensive studies of the mechanics of actomyosin networks have provided great insight on the behavior of the cell cytoskeleton [27, 28]. Microtubule-kinesin suspensions provide quantitative models of the organization and structure of the mitotic spindle [29], but little is known about their rheology.

Here, we report experimental measurements of the shear viscosity of active microtubule nematics. This is obtained by combining (i) experiments on an active MT suspension at an oil-water interface in a set-up that allows us to vary the viscosity of the bounding oil over five orders of magnitude, with (ii) a quantitative analysis of the combined hydrodynamics of the $2d$ active nematic and the bounding bulk passive fluids. By fitting the experimentally measured velocity of topological defects in the active nematic layer to the prediction of the hydrodynamic model that examines the flow induced by nematic textures confined at the interface of two fluids of different viscosity [30–32], we determine an effective bulk shear viscosity of the active nematic and infer the viscosity of the film. Our work yields two important results. First, it shows that activity fluidizes the nematic gel that at the density used in the experiments would be expected to be-

*Electronic address: f.sagues@ub.edu

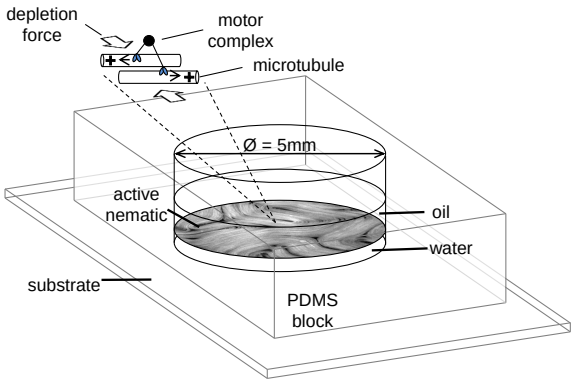

FIG. 1: Experimental setup. The liquids are contained in a cylindrical well custom-engineered on a PDMS block that is bound to a substrate coated with a polymer brush that prevents protein adhesion. The aqueous active material is injected below a volume of silicone oil. Depletion forces promote the formation of the MT bundles, sheared by motor clusters, and lead to the condensation of the active nematic film at the oil/water interface.

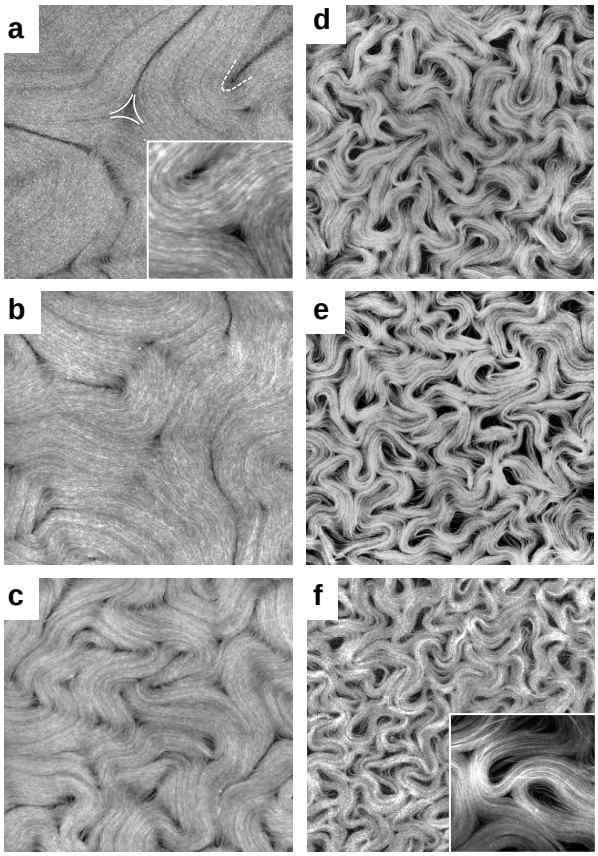

FIG. 2: Active nematic in contact with silicone oils of different viscosity. Fluorescence confocal micrographs are 400μm wide. The oil viscosity, from (a) to (f), is 5×10^{-3}, 5×10^{-2}, 0.5, 5, 12.5, and 300 Pa s, respectively. In frame (a) two streamlines for defects with parabolic ($+1/2$, dashed) and hyperbolic ($-1/2$, solid) morphologies are highlighted. Insets show sections at four-fold magnification.

have like a soft solid, with a finite shear modulus. This echoes early observations in actomyosin gels [33] and is consistent with the expected influence of activity on the rheology of extensile fluids. Secondly, it demonstrates that the rheological characteristics of the interface have a profound effect on the textures and flows of the active nematic, highlighting the need to incorporate the hydrodynamics of bounding fluids so far largely neglected in theoretical models.

The active material we study is based on the hierarchical self-assembly of tubulin into stabilized micron-length fluorescent MTs, organized into bundles that are internally cross-linked and sheared by clusters of kinesin motors [8]. This leads to MT bundle elongation, bending and buckling, which results in extensile local stresses on the surrounding fluid. Once depleted towards a surfactant-decorated oil/water interface, the kinesin/tubulin gel develops the well-known active nematic configuration, which is characterized by self-sustained flows and orientational order of the aligned filaments. Although the thickness of the active nematic layer is not known with precision, we estimate it to be in the range between the minimal bundle thickness, 0.2 μm, estimated from the typical sizes of filaments and motor proteins, and the resolution of fluorescence confocal micrographs, 2 μm. Our open-cell arrangement is based on a custom polydimethylsiloxane (PDMS) block containing a cylindrical well, and bound to a support plate (see Fig. 1 and [34]). After filling the well with silicone oil of the desired viscosity, the aqueous gel is injected between the bottom plate and the oil. This results in an aqueous layer of $100 - 200$ μm depth underneath an oil phase of $1 - 2$ mm depth. Unlike the original arrangement [8], our setup does not demand the use of a low viscosity oil, thus allowing us to explore nearly five orders of magnitude of viscosity contrast between the interfacing oil and the aqueous bulk. In the experiments reported here, ATP concentration is kept at 1.4 mM by means of an enzymatic ATP-regenerator that is incorporated in the active material, which sets a constant activity over the time scale of the experiment.

Results. Because of their extensile nature, MT bundles bend and form parabolic folds, bounding dark regions devoid of MTs (Fig. 2.a). The orientation of the aligned filaments performs half a turn along any closed circuit surrounding either the tip or the tail of the fold. This result allows us to associate a defect topological charge $+1/2$ to the parabolic tip of the fold, and a charge $-1/2$ to the hyperbolic tail. Since the flow originates at the tip of the folds, $+1/2$ defects become like active or self-propelled particles, as first quantified in [35], and can be used as intrinsic tracers for the active flow. On the other hand, $-1/2$ defects often occupy flow stagnation points (see the Supplemental Material [36], Fig. 2). In these nematic films the $+1/2$ defects have also been observed

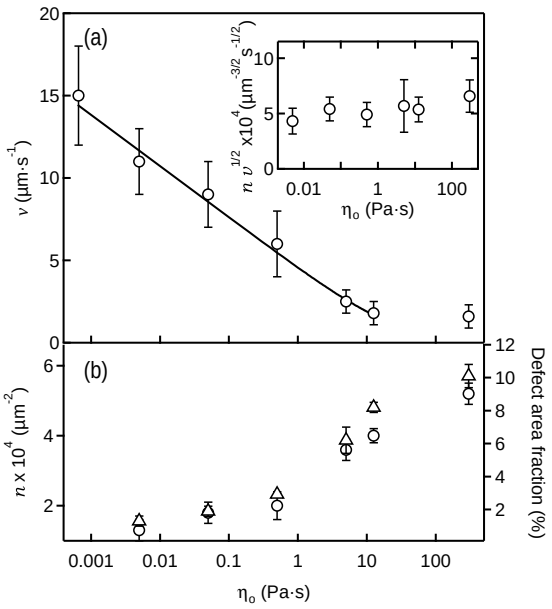

FIG. 3: (a) Average speed of +1/2 defects as a function of oil viscosity. The line is a fit according to the hydrodynamic model described in the text. (b) Defect density (◯) and area fraction covered by defects (△) as a function of oil viscosity. The inset in (a) shows that the combination $nv^{1/2}$ is essentially independent of oil viscosity, as discussed in the text.

to exhibit long-range nematic alignment [37], although the mechanism for such alignment is still controversial [37–39].

Our study has revealed a clear influence of the oil viscosity, η_o, on the morphology and dynamics of the active nematic. In Fig. 2, we show snapshots of the active nematic in contact with oils of different viscosity, for the same activity (i.e., concentration of ATP). These patterns are characterized by the proliferation of randomly moving defects, organizing into the so-called active turbulent regime [35, 40–44]. At higher η_o the number of defects increases and degrades the orientational order of the filament bundles. At the same time, the speed of defects decreases for increasing η_o (see the Supplemental Material [36], Video S1). Textures in contact with oils of smaller viscosity appear less fluorescent (see the Supplemental Material [36], Fig. 3) and more tenuous, as compared to those observed for higher η_o. This indicates that a large η_o concentrates the MT bundles and amplifies the size of the regions void of MTs that we identify with the cores of the defects. Textures such as the one shown in Fig. 2f are rather disordered in the sense that the nematic order parameter would average to a small value. The system, however, still shows a characteristic structure that can be analyzed in terms of nematic disclinations.

We have quantified both the number density, n, and the velocity, v, of the +1/2 defects for the realizations shown in Fig. 2. We observe that v decreases logarithmically with η_o before a saturation is reached for the most viscous oils (Fig. 3a). This data is successfully fitted with the hydrodynamic model described below, which allows us to estimate the viscosity of the active nematic. Conversely, the defect density grows steadily with η_o (Fig. 3b). We have also measured the average size of the defect core, defined as the region devoid of MTs surrounding each defect. We observe that the area fraction occupied by the defect cores is proportional to the defect density, and the average defect core area, which is related to the characteristic defect core size ξ_Q, grows with η_o until saturation for the most viscous oils (see the Supplemental Material [36], Fig. 4).

The measurements of v and n can be combined to reveal a simple scaling relationship between these two quantities. The scaling ansatz can be obtained using generic arguments already proposed for freely suspended active nematics [45]. We assume a simple rate equation for the defect density, $dn/dt = R_c - R_a$, with R_c and R_a the rates of defect creation and annihilation per unit area. The creation rate can be estimated as $R_c \sim (\ell_\alpha^2 \tau)^{-1}$, where $\ell_\alpha = \sqrt{K/|\alpha|}$ is the active length scale determined by balancing active and elastic stresses, with α an active stress scale controlled by ATP concentration and chosen negative for extensile systems. It has been shown that this length scale controls the spatial correlations in the active turbulent regimes of 'wet' active nematics [44, 46]. The time scale $\tau = \gamma/|\alpha|$ controls the relaxation of the order parameter distortions due active stresses, with γ the rotational viscosity of the nematic. The annihilation rate can be estimated as $R_a \sim \sigma v n^2$, with σ an effective cross section (a length in two-dimensions) that quantifies the range of defect interactions. At steady state, the average number density of defects remains constant, giving the scaling prediction $vn^2 \sim \alpha^2/(\gamma\sigma K)$. For a constant ATP concentration, α will be constant, leading to the simplified scaling $vn^2 \sim 1/(\gamma\sigma K)$. Viscous stresses at the interface effectively dampen the active nematic speed (Fig. 3a), which results in more sporadic defect annihilation events. Since the ATP concentration is kept constant in all these experiments, the defect creation rate is sustained. As a result, the number of defects increases (Fig. 3b) while the product $\gamma\sigma K$ is independent of η_o (inset in Fig. 3a).

Hydrodynamic model. To capture the effect of viscous stresses propagated in the nematic by the viscosity contrast at the oil/water interface, we consider the hydrodynamics of a thin active nematic layer confined between two bulk fluids (oil and water) and calculate the velocity that the director distortion due to a +1/2 disclination creates at the core of the defect. Following Ref. [35], and consistently with the analysis of the experiments, we identify this with the defect velocity. We find that the presence of the bulk fluids qualitatively changes the defect velocity as compared to the previously considered cases of a free-standing nematic layer [35, 43], a finite-thickness layer of bulk nematic [42, 47], and a nematic

layer with frictional damping from a substrate [48].

To evaluate the defect velocity, we start with coupled Stokes equations for oil, water and nematic layer,

$$\eta_i \nabla^2 \mathbf{u}_i - \boldsymbol{\nabla} p_i = 0 \ , \quad (1)$$

$$\eta_N \nabla^2 \mathbf{u}_\parallel - \boldsymbol{\nabla}_\parallel p + \hat{\mathbf{n}} \cdot (\boldsymbol{\sigma}_o - \boldsymbol{\sigma}_w) + \boldsymbol{\nabla}_\parallel \cdot \boldsymbol{\sigma}_a = 0 \ , \quad (2)$$

where η_i, $\mathbf{u}_i$ and p_i, with $i = o, w$ denoting oil or water, are the $3d$ viscosity, flow velocity, and pressure of the oil and water subphases respectively; $\boldsymbol{\sigma}_o - \boldsymbol{\sigma}_w$ is the stress jump across the interface, which is projected onto the unit interface normal $\hat{\mathbf{n}}$; η_N, $\mathbf{u}_\parallel$ and p are the $2d$ viscosity, in-plane flow velocity and lateral pressure of the active nematic layer. Finally, $\boldsymbol{\sigma}_a = \alpha \boldsymbol{Q}$ is the active stress arising from the extensile force dipoles exerted by MT bundles on their surroundings and proportional to the nematic alignment tensor $\boldsymbol{Q}$. We neglect elastic stresses that are higher order in gradients in $\boldsymbol{Q}$ than active ones [45]. We compute the nematic flow field $\mathbf{u}_\parallel$ due to stationary textures of the order parameter $\boldsymbol{Q}$ corresponding to either a $+1/2$ or a $-1/2$ defect by solving equations (1) and (2) for an incompressible flow with vanishing of the normal velocity and continuity of the tangential velocity at the nematic interface, located at $z = 0$. Thanks to the linearity of the Stokes equations, the solution is easily written in Fourier space in term of a Green's function. As the depth of both the oil layer and the bulk fluid subphases are much larger than the thickness of the active nematic layer, we consider both bulk layers to be semi-infinite. In this limit, the Fourier components of the flow velocity in the nematic layer are $\mathbf{u}_\parallel(\mathbf{k}) = G(k) \mathcal{P} \mathbf{f}(\mathbf{k})$, where $\mathcal{P} = \boldsymbol{I} - \mathbf{k}\mathbf{k}/k^2$ is a transverse projection operator, $\mathbf{f}(\mathbf{k}) = \int_{\mathbf{r}} e^{-i\mathbf{k}\cdot\mathbf{r}} \boldsymbol{\nabla}_\parallel \cdot \boldsymbol{\sigma}_a$ and the Green's function is given by $G(k) = \left[\eta_N k^2 + \eta_o k\right]^{-1}$ [32]. The length scale $\ell_\eta = \eta_N/(\eta_o + \eta_w) \simeq \eta_N/\eta_o$ (for $\eta_w \ll \eta_o$) controls the crossover from two dimensional surface flows to three dimensional bulk dominated flows.

The scalar order parameter for a $\pm 1/2$ disclination is roughly constant outside the defect core of size ξ_Q, yielding $|\boldsymbol{\nabla} \cdot \boldsymbol{\sigma}_a| \sim |\alpha|/r$ for $r \geq \xi_Q$ [48]. Focusing on the $+1/2$ disclinations, which are motile by virtue of self-induced active backflows [9, 35], the divergence of the active stress $\boldsymbol{\nabla} \cdot \boldsymbol{\sigma}_a$ for a single $+1/2$ disclination has only one non-vanishing component aligned along the axis of the defect (which we freely take to be the x-axis). The velocity at the center of the defect core, assumed to be passively advected by the flow, is then directed along this axis and has a magnitude given by $v = \int'_{\mathbf{r}} G(r) (\boldsymbol{\nabla} \cdot \boldsymbol{\sigma}_a)_x$, where the prime indicates that the integral must be cutoff at small scales by ξ_Q ($\xi_Q \sim 10$ μm from the experimental micrographs), below which the hydrodynamic model ceases to be appropriate, and at a long-wavelength cutoff ℓ controlling the screening of the $2d$ hydrodynamic flows through the coupling to the oil/water subphases. This gives

$$v \simeq \frac{|\alpha|}{\eta_N/\ell} \mathcal{F}_> \left(\frac{\eta_o}{\eta_N/\ell}, \frac{\ell}{\xi_Q} \right) \sim \frac{|\alpha|}{\eta_N/\ell} \ln \left(\frac{\eta_N/\ell}{\eta_o} \right) \ . \quad (3)$$

The exact form of $\mathcal{F}_>$ is given in the SI. The second approximate equality in Eq. (3) holds for $\eta_{\text{eff}} \gg \eta_o$ and $\xi_Q/\ell \ll 1$, with $\eta_{\text{eff}} = \eta_N/\ell$ a three-dimensional viscosity. The logarithmic dependence of v on η_o is robust in these limits and in agreement with the experiments (Fig. 3a). The fit to the data, performed by means of the exact form for v given in the SI, provides a value for $\eta_{\text{eff}} = 13(\pm 5)$ Pa s that depends very weakly on ξ_Q/ℓ for $\xi_Q/\ell < 0.5$ (see SI). Since α is an overall scale for the defect velocity, this analysis gives an essentially parameter free estimate for η_{eff}. On the other hand, the value of η_N depends on ℓ. A natural choice for ℓ is the thickness of the oil subphase ($d \sim 1$ mm) as described in the SI. This gives $\eta_N \sim 13 \times 10^{-3}$ Pa s m. Alternately, one could argue that our single-defect calculation should be cutoff at the scale of the mean defect separation, which in turn depends on η_o (see Fig. 3b), albeit changing only by a factor of two ($50 - 100$ μm) over five decades of oil viscosity. Choosing $\ell \sim n^{-1/2}$, we obtain $\eta_N \sim 6.5 - 13 \times 10^{-4}$ Pa s m over the range of oil viscosities considered.

Importantly, our fit yields $\eta_{\text{eff}}/\eta_o > 1$ at all but the largest oil viscosity ($\eta_o \sim 10^2$ Pa s), where v begins to saturate. We stress that it is *only* in this limit that the defect velocity has a logarithmic dependence on η_o. This physically corresponds to the case when the flow is dominated by the properties of the $2d$ active nematic layer and the bulk fluid only comes as a logarithmic correction to the length scale in the defect velocity. If this ratio were of order unity or smaller, as occurs at the highest value of oil viscosities, then the *qualitative* dependence of the defect velocity on η_o would change, giving $v \sim 1/\eta_o$ instead of the strongly persistent logarithm.

In summary, we have probed the shear viscosity of an active nematic at an oil/water interface using a set-up that allows us to vary the viscosity of the oil by five orders of magnitude. By combining experiments with a hydrodynamic model we show that measurements of the defect velocity can be used to estimate the shear viscosity of the active nematic. An open question is the role of the oil viscosity on the effective elasticity of the active gel. The amplification of the defect cores with increasing oil viscosity suggests an increased effective stiffness, but the decrease of the defect separation suggests the opposite effect. Resolving this discrepancy is a challenging problem that will demand further work.

Acknowledgments

We acknowledge Brandeis MRSEC Biosynthesis facility supported by NSF MRSEC DMR-1420382, and Z. Dogic and S. DeCamp (Brandeis University) for their suport in the preparation of the active gel. We thank B. Hishamunda (Brandeis University), and M. Pons and A. LeRoux (Universitat de Barcelona) for their assistance in the expression of motor proteins. We also thank J. Ortín (Universitat de Barcelona) and R. Casas and G. Valiente (Bluestar Silicones) for providing the silicone oil samples.

MCM was supported by the National Science Foundation through awards DMR-1305184 and DGE-1068780. SS and MCM acknowledge support from the Syracuse Soft Matter Program. P.G. acknowledges funding from Generalitat de Catalunya through a FI-DGR PhD Fellowship. Experiments were funded by MINECO Project FIS 2013-41144P.

[1] M. C. Marchetti, J. F. Joanny, S. Ramaswamy, T. B. Liverpool, J. Prost, M. Rao, and R. A. Simha, Reviews of Modern Physics **85**, 1143 (2013).
[2] S. Ramaswamy, Annual Review of Condensed Matter Physics **1**, 323 (2010).
[3] A. Cavagna, A. Cimarelli, I. Giardina, G. Parisi, R. Santagati, F. Stefanini, and M. Viale, Proc Natl Acad Sci U S A **107**, 11865 (2010).
[4] C. Dombrowski, L. Cisneros, S. Chatkaew, R. E. Goldstein, and J. O. Kessler, Phys Rev Lett **93**, 098103 (2004).
[5] H. P. Zhang, A. Be'er, E. L. Florin, and H. L. Swinney, Proc Natl Acad Sci U S A **107**, 13626 (2010).
[6] V. Schaller, C. Weber, C. Semmrich, E. Frey, and A. R. Bausch, Nature **467**, 73 (2010).
[7] Y. Sumino, K. H. Nagai, Y. Shitaka, D. Tanaka, K. Yoshikawa, H. Chate, and K. Oiwa, Nature **483**, 448 (2012).
[8] T. Sanchez, D. T. Chen, S. J. DeCamp, M. Heymann, and Z. Dogic, Nature **491**, 431 (2012).
[9] V. Narayan, S. Ramaswamy, and N. Menon, Science **317**, 105 (2007).
[10] A. Bricard, J. B. Caussin, N. Desreumaux, O. Dauchot, and D. Bartolo, Nature **503**, 95 (2013).
[11] S. Hernandez-Navarro, P. Tierno, J. A. Farrera, J. Ignes-Mullol, and F. Sagues, Angew Chem Int Ed Engl **53**, 10696 (2014).
[12] W. F. Paxton, K. C. Kistler, C. C. Olmeda, A. Sen, S. K. St Angelo, Y. Cao, T. E. Mallouk, P. E. Lammert, and V. H. Crespi, J Am Chem Soc **126**, 13424 (2004).
[13] J. R. Howse, R. A. L. Jones, A. J. Ryan, T. Gough, R. Vafabakhsh, and R. Golestanian, Physical Review Letters **99**, 048102 (2007).
[14] J. Palacci, S. Sacanna, A. P. Steinberg, D. J. Pine, and P. M. Chaikin, Science **339**, 936 (2013).
[15] H. H. Wensink, J. Dunkel, S. Heidenreich, K. Drescher, R. E. Goldstein, H. Löwen, and J. M. Yeomans, Proceedings of the National Academy of Sciences **109**, 14308 (2012).
[16] A. Majumdar, M. M. Cristina, and E. G. Virga, Philosophical Transactions of the Royal Society of London A: Mathematical, Physical and Engineering Sciences **372**, 20130373 (2014).
[17] A. Sokolov and I. S. Aranson, Physical Review Letters **103**, 148101 (2009).
[18] S. Rafaï, L. Jibuti, and P. Peyla, Physical Review Letters **104**, 098102 (2010).
[19] J. Gachelin, G. Miño, H. Berthet, A. Lindner, A. Rousselet, and É. Clément, Physical Review Letters **110**, 268103 (2013).
[20] H. M. López, J. Gachelin, C. Douarche, H. Auradou, and E. Clément, Physical Review Letters **115**, 028301 (2015).
[21] M. C. Marchetti, Nature **525**, 37 (2015).
[22] Y. Hatwalne, S. Ramaswamy, M. Rao, and R. A. Simha, Physical Review Letters **92**, 118101 (2004).
[23] T. B. Liverpool and M. C. Marchetti, Physical Review Letters **97**, 268101 (2006).
[24] L. Giomi, T. B. Liverpool, and M. C. Marchetti, Phys. Rev. E **81**, 051908 (2010).
[25] G. Henkin, S. J. DeCamp, D. T. Chen, T. Sanchez, and Z. Dogic, Philos Trans A Math Phys Eng Sci **372**, 0142 (2014).
[26] F. C. Keber, E. Loiseau, T. Sanchez, S. J. DeCamp, L. Giomi, M. J. Bowick, M. C. Marchetti, Z. Dogic, and A. R. Bausch, Science **345**, 1135 (2014).
[27] K. E. Kasza, A. C. Rowat, J. Liu, T. E. Angelini, C. P. Brangwynne, G. H. Koenderink, and D. A. Weitz, Current opinion in cell biology **19**, 101 (2007).
[28] C. P. Broedersz and F. C. MacKintosh, Reviews of Modern Physics **86**, 995 (2014).
[29] J. Brugués and D. Needleman, Proceedings of the National Academy of Sciences **111**, 18496 (2014).
[30] P. G. Saffman and M. Delbruck, Proceedings of the National Academy of Sciences **72**, 3111 (1975).
[31] P. G. Saffman, Journal of Fluid Mechanics **73**, 593 (1976).
[32] D. K. Lubensky and R. E. Goldstein, Physics of Fluids **8**, 843 (1996).
[33] D. Humphrey, C. Duggan, D. Saha, D. Smith, and J. Käs, Nature **416**, 413 (2002).
[34] P. Guillamat, J. Ignes-Mullol, and F. Sagues, Proc Natl Acad Sci U S A **113**, 5498 (2016).
[35] L. Giomi, M. J. Bowick, X. Ma, and M. C. Marchetti, Physical Review Letters **110**, 228101 (2013).
[36] See the Supplemental Material at URL ... for a detailed description of the hydrodynamic model used in the manuscript, additional supporting figures, and a supporting video of the experiments.
[37] S. J. DeCamp, G. S. Redner, A. Baskaran, M. F. Hagan, and Z. Dogic, Nat Matter **14**, 1110 (2015).
[38] A. U. Oza and J. Dunkel, New Journal of Physics **18**, 093006 (2016).
[39] A. Doostmohammadi, M. F. Adamer, S. P. Thampi, and J. M. Yeomans, Nat Commun **7**, 10557 (2016).
[40] X. Q. Shi and Y. Q. Ma, Nat Commun **4**, 3013 (2013).
[41] C. A. Weber, C. Bock, and E. Frey, Phys Rev Lett **112**, 168301 (2014).
[42] S. P. Thampi, R. Golestanian, and J. M. Yeomans, Philos Trans A Math Phys Eng Sci **372**, 0366 (2014).
[43] L. Giomi, M. J. Bowick, P. Mishra, R. Sknepnek, and M. Cristina Marchetti, Philos Trans A Math Phys Eng Sci **372**, 0365 (2014).
[44] L. Giomi, Physical Review X **5**, 031003 (2015).
[45] S. P. Thampi, R. Golestanian, and J. M. Yeomans, Phys Rev Lett **111**, 118101 (2013).
[46] E. J. Hemingway, P. Mishra, M. C. Marchetti, and S. M. Fielding, Soft Matter pp. – (2016).
[47] G. Tóth, C. Denniston, and J. M. Yeomans, Physical Review Letters **88**, 105504 (2002).
[48] L. M. Pismen, Phys Rev E Stat Nonlin Soft Matter Phys

88, 050502 (2013).